

PACS numbers: 42.62.Fi; 33.70.-w
DOI: 10.1070/QE2005v035n04ABEH002905

Measurement of the $O_2(b\,^1\Sigma_g^+ \rightarrow a\,^1\Delta_g)$ transition probability by the method of intracavity laser spectroscopy

N.P. Vagin, A.A. Ionin, I.V. Kochetov, A.P. Napartovich,
Yu.P. Podmar'kov, M.P. Frolov, N.N. Yuryshev

***Abstract*. The method of intracavity laser spectroscopy using a Co : MgF_2 laser is applied to record the absorption spectra from the first excited $a\,^1\Delta_g$ state of gaseous molecular oxygen at the $a\,^1\Delta_g \rightarrow b\,^1\Sigma_g^+$ transition at 1.91 μm. The gas flow from a chemical singlet oxygen generator with a known concentration of singlet oxygen O_2 ($a\,^1\Delta_g$) was supplied to the cavity of the Co : MgF_2 laser. The absorption line intensities are measured for five spectral lines of the Q-branch of the 0 – 0 vibrational band for the $a\,^1\Delta_g \rightarrow b\,^1\Sigma_g^+$ transition. The $O_2(b\,^1\Sigma_g^+ \rightarrow a\,^1\Delta_g)$ transition probability calculated from these data was $(1.20 \pm 0.25 \times 10^{-3})$ s^{-1}.**

Keywords: *intracavity laser spectroscopy, Co : MgF_2 laser, singlet oxygen, oxygen – iodine laser.*

1. Introduction

Molecular oxygen $O_2(a\,^1\Delta_g)$ in the first excited electron state, known as singlet oxygen (SO), is an important component of the Earth's upper atmosphere. For example, SO participates in photochemical reactions determining the concentration of ozone in the atmosphere, which protects animals and plants from the action of hard UV radiation from the Sun. An oxygen molecule in the excited state is highly reactive, which is quite important for understanding the role of SO in chemical transformations associated with the pollution of atmosphere, e.g., the processes of formation of nitrogen dioxide [1]. SO also plays an important role in a wide range of biological and medical phenomena [2, 3]. Moreover, it is one of the active components of the active medium in an oxygen – iodine laser [4]. An exact knowledge of the concentration of SO is necessary for understanding the processes occurring with its participation. Hence, methods of detection and quantitative measurement of SO are undoubtedly of considerable interest.

N.P. Vagin, A.A. Ionin, Yu.P. Podmar'kov, M.P. Frolov, N.N. Yuryshev P.N. Lebedev Physics Institute, Russian Academy of Sciences, Leninskii prosp. 53, 119991 Moscow, Russia;
e-mail: frolovmp@x4u.lebedev.ru;
I.V. Kochetov, A.P. Napartovich State Scientific Centre of the Russian Federation 'Troitsk Institute for Innovation and Fusion Research', 142092 Troitsk, Moscow region, Russia

Received 15 October 2004, revision received 4 February 2005
Kvantovaya Elektronika **35** (4) 378 – 384 (2005)
Translated by Ram Wadhwa

From the technical point of view, the simplest among the methods of determining the SO concentration (including the electron paramagnetic resonance [5], absorption spectroscopy in the vacuum ultraviolet (VUV) spectral region [6, 7], etc.) is the one based on the radiation intensity measurement at the $(a\,^1\Delta_g \rightarrow X\,^3\Sigma_g^-)$ transition of O_2 at a wavelength of 1.27 μm [8, 9] with the help of a calibrated photodetector equipped with an appropriate spectral selector (e.g., an interference optical filter). However, absolute calibration of the photodetector is a quite complicated problem and depends to a considerable extent on the measurement geometry, which renders it as a potential source of significant errors. Moreover, the low radiation intensity at the wavelength 1.27 μm due to a low probability of the O_2 $(a\,^1\Delta_g \rightarrow X\,^3\Sigma_g^-)$ transition (the radiative lifetime of such a transition in the gaseous phase is 72 min [10]) considerably hampers such measurements in the presence of background illumination, in particular, during the investigation of an electric discharge in a gas.

These difficulties can be overcome with the help of absorption spectroscopy. For example, the authors of [6, 7] measured the concentration of SO in the gaseous phase from its absorption in the VUV region of the spectrum. Unfortunately, such an approach necessitates the consideration of absorption associated with oxygen molecules in the ground state $O_2(X\,^3\Sigma_g^-)$ since the absorption spectra of SO and unexcited oxygen in the VUV region overlap. This considerably hampers the measurements if the fraction of SO molecules in oxygen is not high.

An alternative absorption method for detection of SO is the measurements of absorption at the $a\,^1\Delta_g \rightarrow b\,^1\Sigma_g^+$ transition lines at 1.91 μm. This transition was observed for the first time by Noxon [11] in the emission spectrum of the electric discharge in a mixture of oxygen and helium. The transition is an electric quadrupole transition [11, 12], and its probability in a gaseous medium is quite low (2.5×10^{-3} s^{-1} [11], 1.7×10^{-3} s^{-1} [13]). Hence, a highly sensitive method must be used for measuring the absorption in this transition.

The intracavity laser spectroscopy (ILS) [14, 15] is one such high-sensitivity absorption technique. The possibility of using the ILS method for detecting SO from absorption at the $a\,^1\Delta_g \rightarrow b\,^1\Sigma_g^+$ transition lines was first demonstrated experimentally in [16]. The Q-branch lines in the 0 – 0 vibrational band of the $O_2(a\,^1\Delta_g \rightarrow b\,^1\Sigma_g^+)$ transition were used for measurements. An estimate of the sensitivity of the setup described in [16] shows that this approach can be used for detecting SO at a concentration level of $\sim 5 \times 10^{14}$ cm^{-3}. A simultaneous recording of several

absorption lines facilitates the identification of the investigated spectrum and makes it possible to measure the temperature of the gaseous medium.

Another advantage of this technique over the method based on the measurement of radiation intensity at the $a\,^1\Delta_g \rightarrow X\,^3\Sigma_g^-$ transition is worth noting. It is well known [17, 18] that the radiation intensity at the $b\,^1\Sigma_g^+ \rightarrow a\,^1\Delta_g$ and $a\,^1\Delta_g \rightarrow X\,^3\Sigma_g^-$ transitions may increase significantly as a result of interaction of $O_2(b\,^1\Sigma_g^+)$ and $O_2(a\,^1\Delta_g)$, respectively, with the molecules of the surrounding gas. In addition to the line spectrum associated with the vibration–rotation structure of levels, the radiation also acquires a diffusion band as a result of molecular interaction. If the resolving power of the spectral instrument used in the investigations is not sufficiently high to single out the line spectrum of the radiative transition, the measurement of the SO concentration from the radiation intensity may lead to overestimated results at high pressures. The main distinguishing feature of the ILS method is the possibility of recording the line absorption spectra, which rules out the errors associated with molecular interaction.

In order to determine the concentration of a substance from absorption spectra, we must know the absorption cross sections of the lines of transitions being studied. For individual lines of the Q-branch, the cross sections can be calculated from the $b \rightarrow a$ transition probability. However, the known data on the probability of this transition are based on the results of the only experimental study [11] (the value 2.5×10^{-3} s^{-1} presented in [11] is obtained to within a factor of 2, while the value 1.7×10^{-3} s^{-1} [13] is also obtained from a repeated estimation of the data presented in [11]). Hence we measured independently in our experiments the absorption line intensities of the Q-branch of the 0–0 vibrational band for the $O_2(a\,^1\Delta_g \rightarrow b\,^1\Sigma_g^+)$ transition and used the obtained results to determine the probability of this transition.

For this purpose, the absorption spectra of SO were recorded by the ILS method using a broad-band $Co : MgF_2$ laser with a known concentration of SO supplied from a chemical singlet oxygen generator (SOG) to its cavity.

2. Experimental setup and the data-processing technique

Experiments were made on the setup described in detail in [16] and modified for operation with a chemical SOG. Figure 1 shows the scheme of the setup. A $Co : MgF_2$ crystal was pumped along the optical axis by a free-running $Nd : YAlO_3$ laser at 1.34 μm. The pump radiation was focused at the centre of the crystal by lens L1. The $Co : MgF_2$-laser pulse duration was 80 – 110 μs. The cavity of the $Co : MgF_2$ laser had a length $L_c = 66$ cm and was formed by a highly reflecting plane mirror M1 and a spherical output mirror M2 ($R = 100$ cm). In order to transform the lasing spectrum of the $Co : MgF_2$ laser, a CaF_2 dispersion prism was installed in the cavity. During operation with SO, the centre of the lasing spectrum was tuned to the wavelength 1.91 μm. The spectral width at the end of the laser pulse was ~ 5 nm.

The $Co : MgF_2$ crystal was placed in a hermetically sealed metallic chamber with the highly reflecting mirror M1 as one of its windows. The output mirror M2 was attached to an external plexiglass flange connected with the chamber through a quartz tube of inner diameter 26 mm. The oxygen supplied by the chemical SOG passed through the quartz tube and entered the evacuation system. The gas flow velocity in the tube was 26 m s^{-1}. Losses during the transportation of SO were minimised due to a low pro-

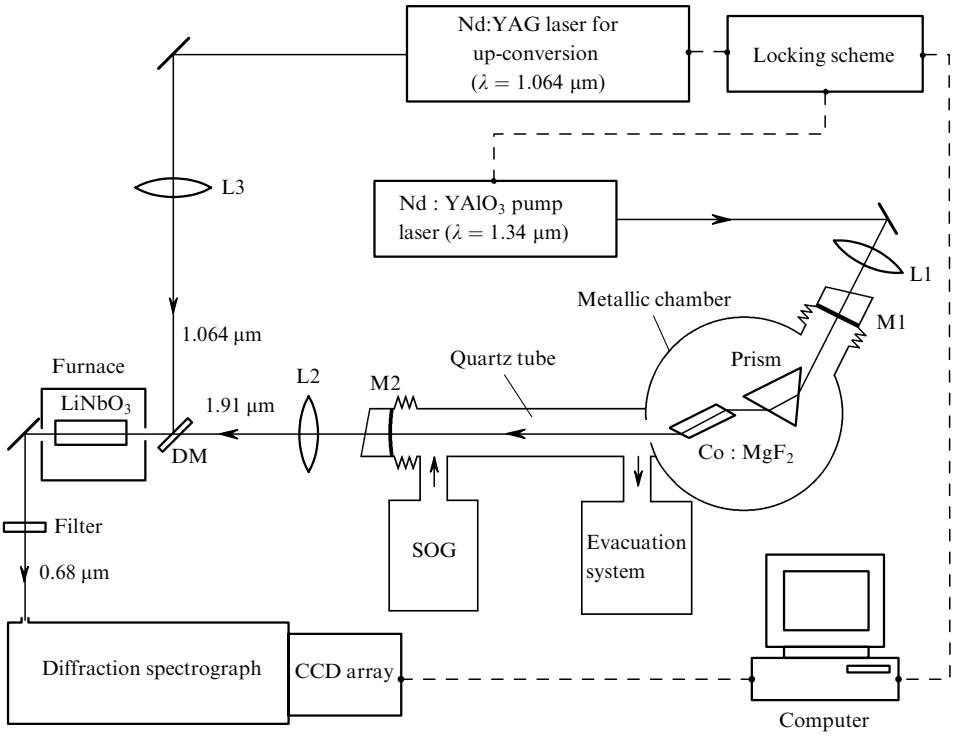

Figure 1. Scheme of the experimental setup: L1, L2, L3 are lenses, M1, M2 are highly reflecting and output mirrors, and DM is a dichroic mirror.

bability of SO quenching at the surface of the plexiglass and quartz, as well as a high rate of circulation. The thickness L_a of the SO absorbing layer in the laser cavity was 30 cm.

The spectral distribution of radiation from the $Co:MgF_2$ laser was recorded with a grating spectrograph (with a spectral resolution of 0.018 cm^{-1}) equipped with an optical multichannel analyser based on a CCD array and connected with a computer. Broadband IR radiation from the $Co:MgF_2$ laser was preliminarily transformed into the visible range ($\lambda \sim 0.68$ μm); for this purpose, it was mixed with monochromatic radiation from a Nd : YAG laser (with $\lambda = 1.064$ μm, linewidth 0.017 cm^{-1}, pulse duration 5 μs, and energy 1 mJ) in a nonlinear $LiNbO_3$ crystal heated in a furnace to approximately 450 °C to attain 90° phase matching. The dichroic mirror DM and lenses L2 and L3 were used for mixing and focusing two laser beams in the nonlinear crystal. Radiation at the sum frequency passed through a filter suppressing radiation at 1.91 and 1.064 μm and was directed to the entrance slit of the spectrograph. To reduce the effect of random fluctuations in the laser spectrum, averaging over 100 laser pulses was performed in each measurement.

The essence of the ILS method can be described as follows. The substance under study with a line absorption spectrum is placed in the cavity of a broadband laser whose lasing band covers the absorption spectrum in which we are interested. If the width of the absorption lines is smaller than the homogeneous width of the gain profile for the active medium in the laser, such a laser operates as a multipass optical cell with an effective absorption length equal to the path length traversed by light in the substance under study during a laser pulse. For this reason, the lasing spectrum of the broadband laser acquires dips that can be described by a modified Bouguer – Lambert – Beer law [15]

$$\frac{I(\omega)}{I_0(\omega)} = \exp\left[-\frac{k(\omega)ctL_a}{L_c}\right], \quad (1)$$

where $I(\omega)$ is the spectral distribution of the lasing intensity as a function of frequency ω at instant t; $I_0(\omega)$ is the envelope of this spectral distribution; $k(\omega)$ is the absorption coefficient; c is the velocity of light; and L_a/L_c is the factor describing the filling of the cavity by the absorbing substance. By measuring the ratio $I(\omega)/I_0(\omega)$ at the absorption line frequency at a preset instant, we can determine the absorption coefficient for this line. If the population of the upper level of the absorbing transition is small, the absorption coefficient is related to the line intensity S and concentration N of absorbing molecules by the expression

$$k(\omega) = SF(\omega)N, \quad (2)$$

where $F(\omega)$ is the absorption line profile normalised to unity. Consequently, knowing the line intensity, we can easily determine the concentration also.

In order to use expression (1) for calculating the molecular concentration, we must write the spectral distribution of radiation emitted by the broadband laser at the specific instant of lasing. For this purpose, an optical shutter is normally used, which makes it possible to single out the required time interval from a laser pulse and to record the corresponding spectral distribution. Here, we took advantage of the fact that the pulse duration of the Nd : YAG laser used for transforming the IR radiation to the visible range was smaller than the duration of a pulse from the $Co:MgF_2$ laser; the locking scheme made it possible to delay the pulse of the Nd : YAG laser for any period of time relative to the leading front of the $Co:MgF_2$-laser pulse. This allowed us to recors the spectral distribution of laser radiation at any instant.

The width of the instrument profile of the recording scheme in our experiments was larger than the width of the oxygen absorption lines, which is determined by Doppler broadening and amounts to 0.0113 cm^{-1} at room temperature. This led to a distortion of the actual profile of the absorption line during the recording and did not allow us to use expression (1) directly for processing the experimental spectra. Hence, in order to obtain quantitative information, we carried out numerical simulation of the absorption spectra for absorbing gas concentrations and effective absorbing length corresponding to the experimental conditions. During simulation, it was assumed that the absorption line profile was described by the Doppler profile, while the instrument profile of the recording scheme was approximated by the diffraction profile of width 0.03 cm^{-1}. Moreover, we also took into account the absorption of the atmospheric air outside the cavity of the $Co:MgF_2$ laser since the laser radiation covered a distance of 70 cm in the atmosphere between the output mirror and the nonlinear $LiNbO_3$ crystal.

By varying the intensities of the SO absorption lines emitted during the experiment and comparing the model spectra with the experimental ones, we attained the best agreement between the experimental and theoretical results. The intensities of lines for which such an agreement was attained, were assigned to the experimental spectra.

3. Approbation of the method

The above method of processing of the experimental results was tested in preliminary experiments in which the absorption spectra of the CO_2 gas were measured in the vicinity of the wavelength 2.003 μm (where the known high-intensity lines of CO_2 are located [19]). For this purpose, the cavity of the $Co:MgF_2$ laser was filled by a prepared mixture of air and CO_2 (concentration of CO_2 in the mixture was 1 %), after which the intracavity absorption spectra were recorded. In these experiments, the filling factor L_a/L_c of the cavity was 0.93. The total pressure p_{mix} of the mixture in the cavity was varied over the range 1 – 15 Torr.

The left-hand side of Fig. 2 illustrates the spectral distribution of the lasing spectrum of the $Co:MgF_2$ laser. These distributions were obtained for a laser pulse duration of 80 μs and $p_{mix} = 0.9$, 1.9 and 3.8 Torr. The dips observed in the lasing spectra are associated with the water vapour lines (marked by dark squares) and CO_2 lines [19].

The right-hand side of Fig. 2 shows the results of numerical simulation of the spectral distribution of radiation passing through a layer of atmospheric air enriched with CO_2 gas, under the same pressures and for an absorption layer thickness of 22.3 km (effective path length). During simulation, the instrument function of the recording scheme was taken into account, and the frequencies and intensities of CO_2 and H_2O lines were borrowed from the HITRAN 2004 data base [19]. It was assumed that the initial emission spectrum is described by the envelope of the corresponding experimental laser

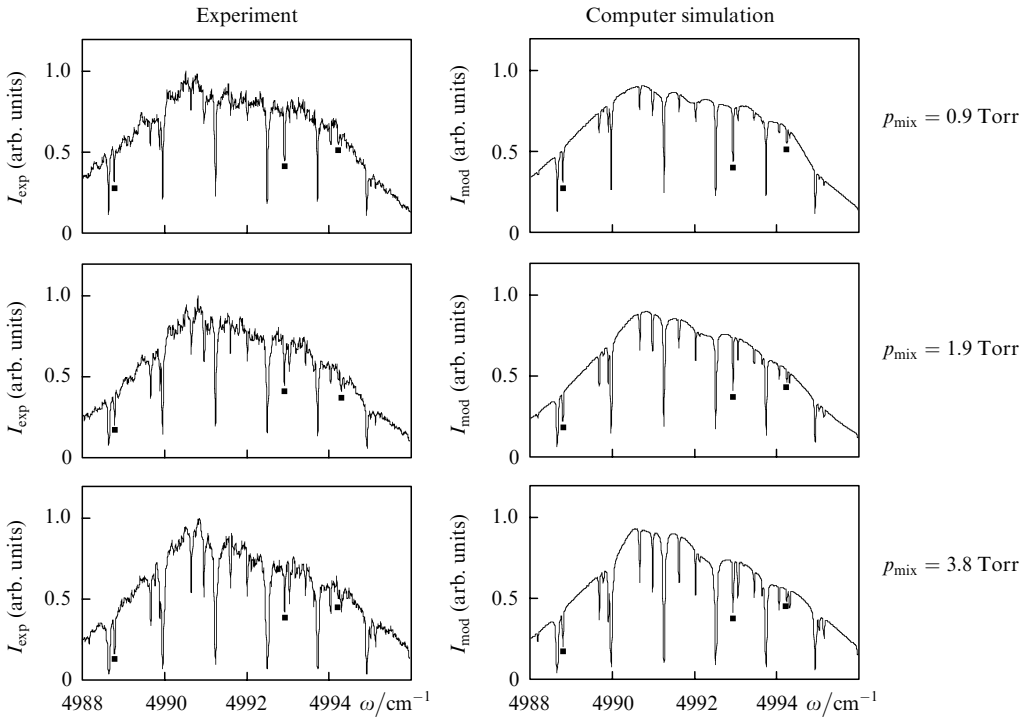

Figure 2. Spectral distributions of radiation from Co : MgF_2 laser, recorded during the filling of cavity with air enriched with CO_2 to a concentration of 1 % (left), and corresponding results of numerical simulation of the spectral distribution of radiation passing through a layer of atmospheric air enriched with CO_2 under the same pressure and for an absorbing layer thickness of 22.3 km taking into account the instrument function of the recording scheme and experimental envelope of the lasing spectrum (right). Squares mark the water vapour lines.

radiation spectrum. It was assumed during simulation that concentration of CO_2 in the mixture was 1 %. As regards the water vapour, the experimental measurements show that a certain background level of water vapour is always present in the cavity, but its concentration cannot be controlled in our experiments. Hence during simulation we chose such partial pressures of water vapour for which the best agreement between the experimental and model spectra was attained. The model spectra presented in Fig. 2 were obtained for a water vapour pressure of 0.007 Torr.

An analysis of the obtained results shows that a good agreement between the experimental and theoretical absorption spectra of CO_2 is attained in all cases. In our opinion, this is a sound argument in favour of using the above procedure for processing of spectra.

4. Measurement of the SO absorption line intensity

In order to measure the absorption line intensity of the Q-branch of the 0–0 vibrational band for the molecular oxygen transition $a\,^1\Delta_g \rightarrow b\,^1\Sigma_g^+$, we carried out a series of experiments in which the ILS method was used to record the absorption spectra of the gaseous mixture supplied to the cavity of the Co : MgF_2 laser from a bubbling chemical SOG, and containing SO with a known partial pressure.

Such a generator having a diameter of 150 mm was used earlier [20] for studies involving a pulsed oxygen–iodine laser (OIL). In this work, detailed investigations of the dependence of SO yield on the working parameters of the generator were carried out. The threshold technique was used for determining the SO yield. This method involves the dilution of the flow containing SO with unexcited oxygen until lasing in the pulsed OIL is disrupted. According to the working principle of the OIL, the concentration of SO at the disruption point $Y = [O_2(a\,^1\Delta_g)]/[O_2]$ is equal to the threshold concentration $Y_{th} = [1 + 1.5\exp(402/T)]^{-1}$, where $[O_2(a\,^1\Delta_g)]$ is the SO concentration, $[O_2]$ is the total concentration of oxygen, and T is the gas flow temperature in degrees Kelvin. It is found that $Y_{th} = 15\,\%$ at room temperature. Knowing the flow temperature and the flow rate of the mixture as well as the added oxygen, we can easily find the concentration of SO in the flow being studied, and hence the overall concentration of SO. Our measurements reveal that for an oxygen pressure of 1 Torr in the laser cell and an evacuation rate of ~ 100 L s^{-1}, the SO concentration is equal to 50 %. The relative error in determining the SO concentration is 15 %.

Since the evacuation rate in our experiments was 14 L s^{-1} and the diameter of the SOG was 100 mm, the concentration of SO was determined by measuring the luminescence signal at the $O_2(a\,^1\Delta_g \rightarrow X\,^3\Sigma_g^-)$ transition at a wavelength of 1.27 μm in a specially prepared measuring unit initially calibrated to a SOG of diameter 150 mm. To reduce the concentration of water vapour resulting from the use of aqueous solutions of reagents in the flow emerging from the SOG, a low-temperature trap cooled by ethyl alcohol to a temperature of −70 °C was mounted in the gas duct downstream from the SOG. Buffer gas (air) was added to the flow in order to maintain a constant rate of evacuation upon a variation of SO pressure.

The method described above made it possible to supply to the cavity a flow of gas containing SO under partial pressure up to 0.5 Torr. The error in determining the SO concentration did not exceed 15 %.

We carried out five series of experiments, and absorption

spectra for the products of chemical SOG under partial SO pressures p_{SO} in the cavity equal to 0.14, 0.20, 0.26, 0.35 and 0.42 Torr were recorded in each case. In each series of experiments, the absorption spectrum was obtained as a result of averaging over 100 measurements. The left-hand side of Fig. 3 shows some of the experimental transmission spectra T_{exp} of the gas flow emerging from a chemical SOG (partial pressures of SO are shown on the right). The lower spectrum was obtained in the absence of SO in the gas flow (blowing of air through the SOG). Each of the spectra shown in the diagram was obtained by dividing the recorded spectral distribution of laser radiation by the envelope of this spectrum. The overall pressure of oxygen and the buffer gas in the cavity was 2.2–3.3 Torr. The Doppler broadening of lines dominates under such pressures. The lasing pulse duration in the $Co:MgF_2$ laser was 90 μs.

In order to identify the SO lines, we used the data of Ref. [12]. In the spectral region shown in Fig. 3, seven SO lines fall in the 0–0 band with rotational numbers J assuming even values from 2 to 14. In addition to the SO lines, the spectrum also contains a large number of water vapour lines [19], some of which overlap strongly with the singlet oxygen lines Q(2) and Q(8) which are thus rendered unsuitable for the purpose of data processing. The remaining five SO lines virtually do not overlap with the water lines and may be used for measurement. These lines are marked in Fig. 3 by circles, and their frequencies are presented below in Table 1.

The right-hand side of Fig. 3 shows model transmission spectra T_{mod} of the chemical SOG products for an absorbing layer thickness of 12.3 km (the distance covered by light during 90 μs for a cavity filling factor $L_a/L_c = 30/66$). In the course of simulation, it was assumed that SO and the accompanying water vapour are responsible for the absorption. Unfortunately, the data contained in the HITRAN 2004 base on weak H_2O absorption lines in the spectral range studied by us are apparently neither complete nor quite accurate. Moreover, it cannot be ruled out that the gas flow emerging from the chemical SOG may contain not only water vapour, but also the absorbing impurity about which no information is contained in the HITRAN data base. Hence, we supplemented the data from the HITRAN base by the results of our own measurements. This allowed us to obtain model absorption spectra matching with the experimental spectra. The partial pressure of water vapour in calculations was 0.1–0.2 Torr. A more detailed analysis of the absorption spectra of water vapour and other impurities is beyond the scope of this study.

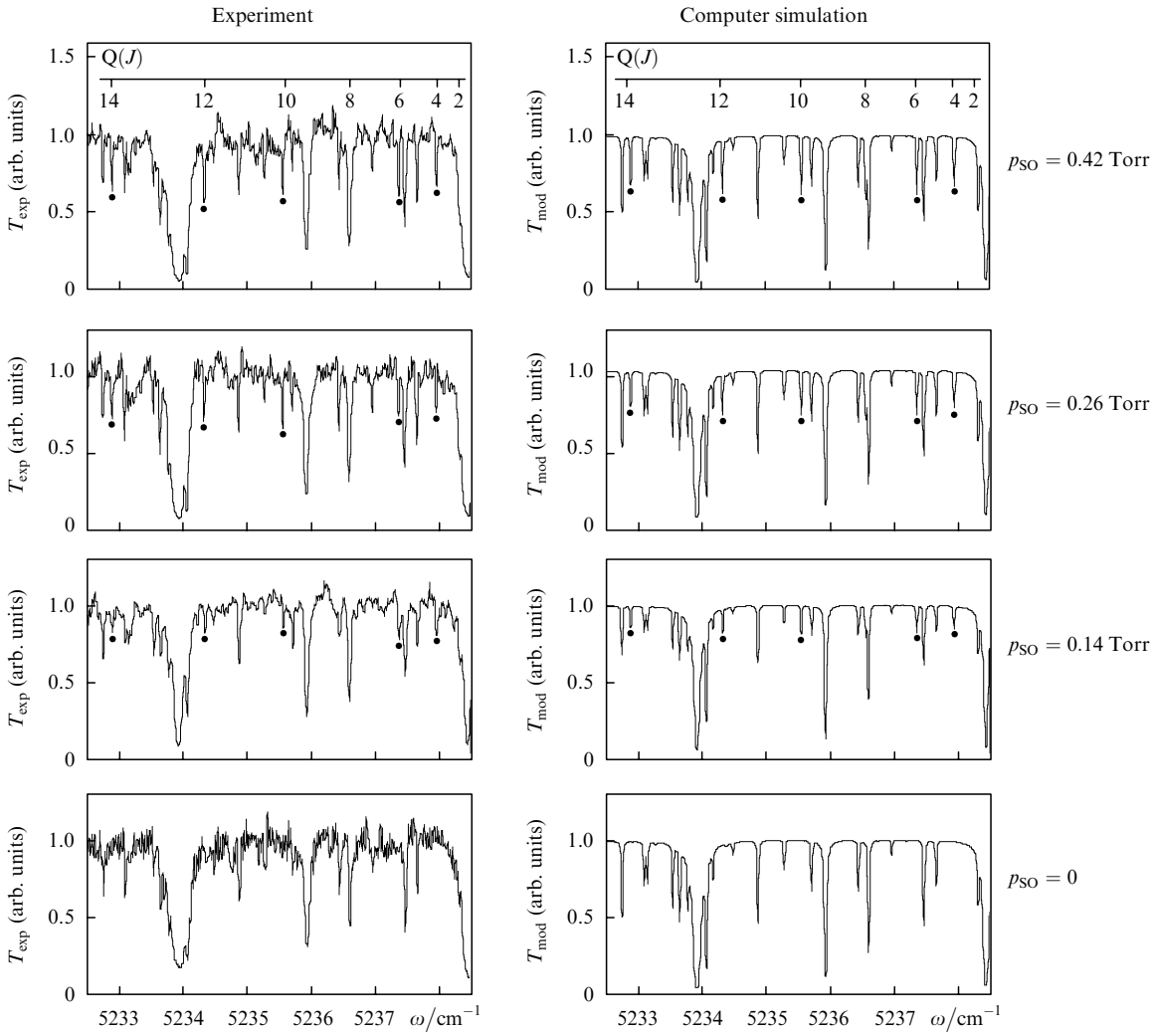

Figure 3. Experimental transmission spectra of the chemical SOG products (left) and the corresponding model transmission spectra of SO and water vapour (right) obtained for various partial pressures of SO. The SO lines used for measurements are marked by circles.

Table 1.

J	ω/cm^{-1} [12]	$p_{SO} = 0.14$ Torr, $p = 2.15$ Torr		$p_{SO} = 0.20$ Torr, $p = 2.29$ Torr		$p_{SO} = 0.26$ Torr, $p = 3.24$ Torr		$p_{SO} = 0.35$ Torr, $p = 2.68$ Torr		$p_{SO} = 0.42$ Torr, $p = 3.30$ Torr	
		$S_J/10^{-24}$ cm	$A_{b\to a}/10^{-3}\,s^{-1}$	$S_J/10^{-24}$ cm	$A_{b\to a}/10^{-3}\,s^{-1}$	$S_J/10^{-24}$ cm	$A_{b\to a}/10^{-3}\,s^{-1}$	$S_J/10^{-24}$ cm	$A_{b\to a}/10^{-3}\,s^{-1}$	$S_J/10^{-24}$ cm	$A_{b\to a}/10^{-3}\,s^{-1}$
4	5237.944	1.00	1.04	1.10	1.25	1.20	1.39	1.10	1.19	1.10	1.18
6	5237.359	1.50	1.25	1.45	1.30	1.30	1.19	1.10	0.95	1.30	1.11
10	5235.550	1.20	0.98	1.35	1.14	1.70	1.44	1.15	0.95	1.20	0.99
12	5234.325	1.30	1.22	1.40	1.31	1.50	1.41	1.20	1.12	1.20	1.12
14	5232.885	1.00	1.16	1.20	1.34	1.20	1.34	1.00	1.14	1.00	1.15
$A^{(m)}_{b\to a}/s^{-1}$		1.13×10^{-3}		1.27×10^{-3}		1.35×10^{-3}		1.07×10^{-3}		1.11×10^{-3}	
T/K		302 ± 33		335 ± 28		343 ± 33		317 ± 45		312 ± 21	

Note: S_J is the absorption line intensity and $A^{(m)}_{b\to a}$ are the mean values of the Einstein coefficients for the $b \rightarrow a$ transition.

Our estimates based on the measurements of radiation intensity of oxygen at the transition $b\,^1\Sigma_g^+ \rightarrow X\,^3\Sigma_g^-$ in the vicinity of the wavelength 760 nm show that the population of the $O_2(b\,^1\Sigma_g^+)$ state did not exceed 10^{13} cm^{-3} in all our experiments, which is negligible compared to the population of the $O_2(a\,^1\Delta_g)$ state. Hence, the population of the $O_2(b\,^1\Sigma_g^+)$ state was assumed to be zero in our simulation.

It was also assumed that all molecules in the $O_2(a\,^1\Delta_g)$ state are at the zero vibrational level. The justification of such an assumption follows, for example, from [21] where it was shown that the vibrational population of SO emerging from a chemical drop-jet SOG is 2 %. Our own measurements of intensity of dimole radiation in the processes

$$O_2(a\,^1\Delta_g, v = 0) + O_2(a\,^1\Delta_g, v = 0)$$

$$\rightarrow 2O_2(X\,^3\Sigma_g^-, v = 0) + h\nu\ (\lambda = 634\ \mathrm{nm}),$$

and

$$O_2(a\,^1\Delta_g, v = 1) + O_2(a\,^1\Delta_g, v = 0)$$

$$\rightarrow 2O_2(X\,^3\Sigma_g^-, v = 0) + h\nu\ (\lambda = 579\ \mathrm{nm})$$

also show that the fraction of vibrationally excited SO in a bubble SOG does not exceed a few percent. The results of processing of the obtained data are presented in Table 1.

5. Probability of the $O_2(b\,^1\Sigma_g^+ \rightarrow a\,^1\Delta_g)$ transition

The expression ($K \equiv \int k(\omega)\mathrm{d}\omega$) for the integrated absorption coefficient for an isolated Q-branch line of the 0–0 vibrational band for the $a\,^1\Delta_g \rightarrow b\,^1\Sigma_g^+$ transition in the case of an equilibrium distribution over rotational levels has the form [22–24]

$$K_J = \frac{\lambda^2}{8\pi c} A_{JJ} \frac{g_b}{g_a} N_{a,J}, \tag{3}$$

where λ is the transition wavelength; A_{JJ} is the probability of spontaneous emission from $O_2(b\,^1\Sigma_g^+, v = 0, J)$ to $O_2(a\,^1\Delta_g, v = 0,\ J)$; $g_a = 2$, $g_b = 1$ are the degeneracy factors of the electron states $a\,^1\Delta_g$ and $b\,^1\Sigma_g^+$; and $N_{a,J}$ is the population at the O_2 level ($a\,^1\Delta_g, v = 0, J$) (the population of the upper $b\,^1\Sigma_g^+$ state is negligibly low).

Since the Frank–Condon factor for the band under consideration is close to unity ($q_{00} = 0.977$ [13]), the contribution from the remaining vibrational bands can be disregarded in the subsequent analysis. The dependence of A_{JJ} on J is described by the Hönl–London factor S_{JJ}. For the Q-branch of the 0–0 vibrational band for the electric quadrupole transition $a\,^1\Delta_g \rightarrow b\,^1\Sigma_g^+$, the expression for the Hönl–London factor was derived in [25] (see also [26]):

$$S_{JJ} = \frac{2(2J+1)(J+2)(J-1)}{(2J-1)(2J+3)}.$$

For $J > 2$, this quantity can be approximated to a good degree of precision by the expression $S_{JJ} \approx (2J+1)/2$. Normalisation (sum) of the Hönl–London factors for the quadrupole transition $^1\Delta_g \rightarrow {}^1\Sigma_g^+$ is presented in [27] and is equal to $(4/3)(2J+1)$. The Einstein coefficient $A_{b\to a}$ (probability of the $b\,^1\Delta_g \rightarrow a\,^1\Sigma_g^+$ transition) is determined by the contribution from five branches (O, P, Q, R, S) whose intensity ratio was derived theoretically in [25] and verified experimentally in [12]. For $J > 2$, the fraction of the Q-branch in which we are interested is equal to 3/8. Thus, formula (3) can be written by using the Einstein coefficient $A_{b\to a}$ in the form

$$K_J = \frac{\lambda^2}{8\pi c}(3/8) A_{b\to a} \frac{g_a}{g_a} N_{a,J}. \tag{4}$$

For the $O_2(a\,^1\Delta_g, v = 0)$ state, the population density of the rotational levels [23, 24] is defined as

$$N_{a,J} = \frac{g_I^{a,s}(2J+1)}{Q_I Q_r} N_a \exp\left[-\frac{B_a}{T} J(J+1)\right], \tag{5}$$

where $g_I^{a,s}$ is the nuclear statistical weight for antisymmetric and symmetric states respectively; Q_I is the nuclear statistical sum; Q_r is the rotational statistical sum; N_a is the total population of the level $a\,^1\Delta_g$; $B_a = 1.4178402$ cm^{-1} [12] is the rotational constant; and T is the absolute temperature in cm^{-1}. Because the spin of O nucleus in the homonuclear molecule $^{16}O_2$ is equal to zero, we obtain $g_I^a = 0$ (antisymmetric state) and $g_I^a = 1$ (symmetric state). However, the nuclear statistical weights in the state $a\,^1\Delta_g$ are identical for rotational levels with odd and even J, since a symmetric wavefunction exists for each $J \geqslant \Lambda = 2$ as a result of Λ-doubling ($Q_I = 1/2$). The rotational partition function Q_r is equal to $\sum (2J+1)\exp[-B_a J(J+1)/T] \approx T/B_a$.

It follows from expression (2) that $K_J = S_J N_a$. Taking this fact into account, we obtain from (4), (5) an expression

relating the intensity S_J of the absorption lines with the transition probability $A_{b\to a}$:

$$S_J = \frac{3\lambda^2}{64\pi c} A_{b\to a} \frac{B_a}{T}(2J+1)\exp\left[-\frac{B_a}{T}J(J+1)\right]. \qquad (6)$$

Because this expression contains the temperature, hence we must know the temperature of the gas flowing in the cavity in order to calculate the transition probability from the measured line intensities. It was mentioned above that we were able to make measurements simultaneously for five absorption lines of SO. It follows from (6) that $\ln[S_J/(2J+1)] = -(B_a/T)[J(J+1)] + \text{const}$, i.e., the dependence of the function $\ln[S_J/(2J+1)]$ on $J(J+1)$ has the form of a straight line whose slope is determined by the rotational temperature. Having constructed the corresponding dependences and assuming the equality of rotational and translational temperatures, we determined the temperature T of the gaseous mixture in the cavity for each series of measurements (see Table 1). The temperature of the gas flow changes due to cooling in the low-temperature trap and subsequent heating as a result of heat exchange with the walls and heat release due to SO relaxation. Since there is no noticeable correlation between the temperature and pressure of the SO, it can be assumed that the flow thermalisation with the walls is the dominant process, i.e., we can assume that the temperature of the flow is equal to room temperature.

Proceeding from the values obtained for line intensities and temperature and using expression (6), we determined the transition probabilities $A_{b\to a}$ for each series of measurements (see Table 1). The second line from below in Table 1 contains values of $A^{(m)}_{b\to a}$ averaged over each series. The value of $A_{b\to a}$ averaged over the entire body of data was $(1.20 \pm 0.25) \times 10^{-3}$ s^{-1}.

While measuring the transition probability, the author of [11] assumed that the intensity of the Q-branch is 1/5 of the total intensity of the 0–0 band. However, more recent data [12, 25] indicate that the Q-branch intensity is $3/8 = 0.375$ of the total intensity. Hence, the value 1.7×10^{-3} s^{-1} given in [13] should be multiplied by the coefficient 0.2/0.375; this leads to the value 0.91×10^{-3} s^{-1}, which is in good agreement with our results. The radiative lifetime of the $a\,^1\Delta_g \to b\,^1\Sigma_g^+$ transition calculated by the authors of [28] was found to be 720 s, which corresponds to a transition probability of 1.39×10^{-3} s^{-1}. This value is also close to the value obtained in our measurements.

6. Conclusions

We have measured in this study the intensities of five lines in the Q-branch of the 0–0 vibrational band of the electric quadrupole $a\,^1\Delta_g \to b\,^1\Sigma_g^+$ transition of molecular oxygen and determined the probability of this transition. This makes it possible to use the ILS method for absolute quantitative measurements of the SO concentration, e.g., in the studies of new sources of singlet oxygen.

Acknowledgements. The work was supported by AFRL, EOARD and the International Science and Technology Centre (Project No. 2415R) and by the President of the Russian Federation Grant No. NSh-794.2003.2.

References

1. Wayne P.R., in *Advances in Photochemistry* (New York–London–Sidney–Toronto: Interscience Publ., 1969) Vol. 7, p. 311.
2. Zakharov S.D., Ivanov A.V. *Kvantovaya Elektron.*, **29**, 192 (1999) [*Quantum Electron.*, **29**, 1031 (1999)].
3. Kamalov V.F., Stepanova N.V., et al. *Kvantovaya Elektron.*, **12**, 1997 (1985) [*Sov. J. Quantum Electron.*, **15**, 1319 (1985)].
4. McDermott W.E., Pchelkin N.R., Benard D.J., Bousek R.R. *Appl. Phys. Lett.*, **32**, 469 (1978).
5. Richardson J., Wiswall C.E., et al. *J. Appl. Phys.*, **52**, 4962 (1981).
6. Sharpless R.L., Slanger T.G. *J. Chem. Phys.*, **91**, 7947 (1989).
7. Coxon J.A., Roychowdhury U.K. *Appl. Spectrosc.*, **52**, 203 (1986).
8. Krasnovskii A.A. Jr. *Biofizika*, **21**, 748 (1976).
9. McDermott W.E., Pchelkin N.R. *Rev. Sci. Instrum.*, **49**, 794 (1978).
10. Miller H.C., McCord J.E., Choy J., Hager G.D. *J. Quantum Spectr. Rad. Transfer*, **69**, 305 (2001).
11. Noxon J.F. *Can. J. Phys.*, **39**, 1110 (1961).
12. Fink E.H., Kruse H., Ramsay D.A., Vervloet M. *Can. J. Phys.*, **64**, 242 (1986).
13. Krupenie P.H. *J. Phys. Chem. Ref. Data*, **1**, 423 (1972).
14. Pakhomycheva L.A., Sviridenkov E.A., Suchkov A.F., Titova L.V., Churilov S.S. *Pis'ma Zh. Eksp. Teor. Fiz.*, **12**, 60 (1970).
15. Baev V.M., Latz T., Toschek P.E. *Appl. Phys. B*, **69**, 171 (1999).
16. Pazyuk V.S., Podmarkov Yu.P., Raspopov N.A., Frolov M.P. *Kvantovaya Elektron.*, **31**, 363 (2001) [*Quantum Electron.*, **31**, 363 (2001)].
17. Fink E.H., Setzer K., et al. *Int. J. Quantum Chem.*, **39**, 287 (1991).
18. Wildt J., Fink E.H., Biggs P., Wayne R.P., Vilesov A.F. *Chem. Phys.*, **159**, 127 (1992).
19. The HITRAN database, 2004 edition (www.hitran.com).
20. Vagin N.P., Pazyuk V.S., Yuryshev N.N. *Kvantovaya Elektron.*, **22**, 776 (1995) [*Quantum Electron.*, **25**, 746 (1995)].
21. Azyazov V.N., Nikolaev V.D., Svistun M.I., Ufimtsev N.I. *Kvantovaya Elektron.*, **28**, 212 (1999) [*Quantum Electron.*, **29**, 767 (1999)].
22. Mitchell A.C., Zemansky W.M. *Resonance Radiation and Excited Atoms* (New York: Cambridge Univ. Press, 1961).
23. Kuznetsova L.A., Kuz'menko N.E., Kuzyakov Yu.Ya., Plastinin Yu.A. *Veroyatnosti opticheskikh perekhodov dvukhatomnykh molekul* (Probabilities of Optical Transitions in Diatomic Molecules) (Moscow: Nauka, 1980) Ch. 2.
24. Kuznetsova L.A., Surzhikov S.T., in *Entsiklopediya nizkotemperaturnoi plazmy* (Encyclopaedia of Low-temperature Plasmas) Ed. by Fortov V.E. (Moscow: Nauka/Interperiodika, 2000) p. 376.
25. Chiu Y.N. *J. Chem. Phys.*, **42**, 2671 (1965).
26. Kovacs I. *Rotational Structure in the Spectra of Diatomic Molecules* (London: Adam Hilger Ltd., 1969) p. 124.
27. Whiting E.E., Paterson J.A., Kovacs I., Nichols R.W. *J. Mol. Spec.*, **47**, 84 (1973).
28. Klotz R., Marian C.M., Peyerimhoff S.D. *Chem. Phys.*, **89**, 223 (1984).